Enhancing the Signal-to-Noise Ratio in Optically Pumped Cesium Beam Tubes Using a Hexapole Magnetic System

Yufei Yan, Haijun Chen, Jinjun Feng
National Key Laboratory of Science and Technology on Vacuum Electronics
Beijing Vacuum Electronics Research Institute
Beijing, China
yufeiyan1003@163.com

Duo Pan, Tianyu Liu, Jingbiao Chen
State Key Laboratory of Advanced Communication System and Networks, Department of Electronics, Institute of Quantum Electronics
Peking University
Beijing, China
panduo@pku.edu.cn

***Abstract*—In order to improve the currently limited Signal-to-Noise Ratio (SNR) of the compact optically pumped cesium beam tubes, we proposed a hexapole magnetic focusing method for the cesium beams. The total number of the detected cesium atoms with a hexapole magnetic system were calculated and found to be 9.5 times higher than that without the hexapole magnetic system. This result gives a prediction of 3.1 fold increase in the SNR when only the shot noise is considered, compared with the conventional tubes. In order to be closely integrated with experimental verification, the hexapole magnetic system was engineered and the simulation results of this structure shown that it not only met the magnetic induction requirements of the simulation under multiple channels, but also had effective magnetic shielding.**

Keywords—Atomic clock; Optical pumping; Cesium beam tube; Hexapole magnetic focusing; Signal-to-Noise Ratio; Frequency stability

I. INTRODUCTION

In virtue of the high frequency accuracy, the cesium beam standards that provide the precise time and frequency information, have been widely used in navigation, communications, calibration laboratories, and a variety of scientific endeavors.[1],[2] Since the 1950s, the magnetic state-selecting primary cesium clocks were developed rapidly, such as NBS-6 of NIST in the United States and CS2 of PTB in Germany.[3]-[6] The commercialized cesium atomic clock 5071A, has a short-term frequency stability better than 8.5×10^{-13} at the sampling time of 100 seconds by using a high performance tube, and has been one of the most important frequency standards at time and frequency laboratories around the world.[7]-[9] The magnetic state-selecting cesium clocks, however, are facing a great challenge to improve their atom utilization since nearly half of the atoms are spatially deflected by the magnetic field from the state selector magnet A.[10]-[13]

Meanwhile, an application of optical pumping state preparation, in conjunction with fluorescence detection, enable a larger number of cesium atoms can be utilized.[14]-[16] For example, NIST-7, an optical pumped, a replacement of NBS-6, served as the primary time and frequency standard in the United States from 1993 to 1999. Its frequency stability characterized by $\sigma_y(\tau)=8\times10^{-13}\tau^{-1/2}$, is an order of magnitude higher than the magnetic state-selecting primary frequency standard.[17]-[19] As a merchandised product, TA1000, with performance comparable to 5071A, has been used in recent years.[20] Benefiting from the state-of-the-art high-stability 852nm laser, the frequency stability of a compact optically pumped cesium atomic clock has reached $2\times10^{-12}\tau^{-1/2}$.[21]

For the compact optically pumped cesium clocks used in the engineering fields, their performance indicators, such as the frequency stability, seem to have reached a plateau due to their limited volume. It is well known that the performance of these clocks can be improved directly and effectively by increasing the utilization efficiency of cesium atoms. To do so, we propose a focusing method for the cesium atoms with large emission angles by adding a hexapole magnetic system between the pumping region and the microwave cavity. The total number of the cesium atoms per second detected at the detecting region, were calculated and simulated for the single and multiple beam channel configurations, respectively, to verify the effectiveness of the proposed method.

In Sec. II, we describe the method of using a hexapole magnetic system to focus atoms with large emission angles. Section III is the description of the calculation and simulation methods, their results of the detected atomic beam flux and atomic trajectories were also shown in this section. In Sec. IV, the solid model of the hexapole magnetic system was engineered, and the simulation results verified the validity and rationality of the designed structure.

II. METHODS

Fig. 1(a) illustrates the physical scheme of the optically pumped cesium beam frequency standards using a hexapole magnetic system, which consists of a cesium oven, pumping laser, hexapole magnetic system, microwave cavity and detecting laser. The cesium atoms, generated by the cesium oven, has the ground states of F=3 and F=4. For the preparation of the F=4 state, the atoms with the F=3 state are pumped to the excited states, ending up with the F=4 state, with the pumping laser tuned to the optical transition

978-1-6654-3935-0/21/$31.00 ©2021 IEEE

$F=3\rightarrow F'=3$ or $F=3\rightarrow F'=4$. These atoms of the F=4 state are then focused in the hexapole magnetic system. As shown in Fig. 1(b), the six poles are paired in polarity and distributed uniformly to form a circular cross section. The expression of the magnetic induction B in the hexapole magnet is given by:[2]

$$B = B_0(\frac{r}{r_0})^2 \tag{1}$$

where B_0 represents the magnetic induction at the pole cone end, r is the radial position of cesium atoms with respect to the bore center of the hexapole magnetic system, and r_0 is the bore radius of the hexapole magnetic system. The deflection force exerted on the atoms with different hyperfine states in the hexapole magnetic field is expressed as:

$$F = \pm 2\mu_{eff} B_0 \frac{r}{r_0^2} \tag{2}$$

where μ_{eff} is effective magnetic moment.[22] The states of (3, m_F) and (4, -4) carry the positive sign, while all the high energy (4, m_F) states except (4, -4) carry the negative sign, which will be focused in a magnetic field. In fact, it has been confirmed in the study of hydrogen atomic clocks that atoms with high energy levels can be focused by the hexapole magnet.[23],[24] Then the focused beams enter into the U-shaped microwave cavity, the cesium atoms of F=4, m_F=0 state, excited by the RF signal, undergo a clock transition to the F=3, m_F=0 state. Finally, the atoms of the F=3, m_F=0 state were detected by the detecting laser, which is locked to the optical cycling transition $F=3\rightarrow F'=2$, as seen from Fig. 1(c). It is worth noting that the locked frequency of the pumping and detecting lasers with 852nm wavelength used here are different from the conventional optically pumped cesium beam frequency standards.[25]-[29]

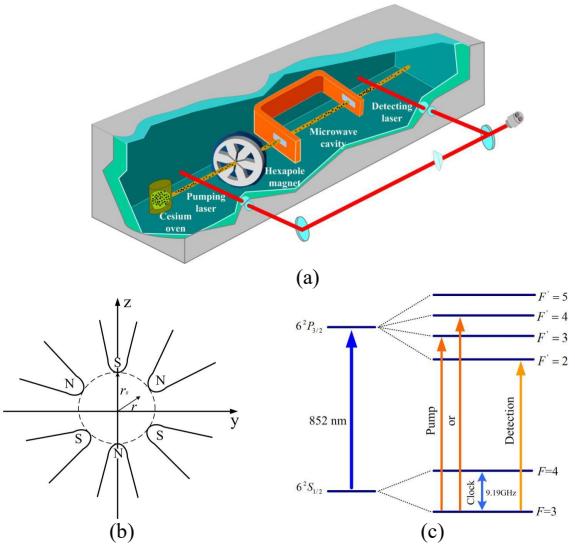

Fig. 1. (a) Physical scheme of optically pumped cesium beam frequency standard using a hexapole magnetic system. (b) Cross section view of the hexapole magnetic system. (c) Relevant energy levels transition of a cesium atom.

III. The Calculations of I_{ATOM} and Atomic Trajectories

The atomic beam flux $I(\theta)$ at one unit solid angle is related to the emitting angle θ between the moving direction of an atom and the axis direction of the oven nozzle aperture, and can be expressed as:[30]

$$I(\theta)=\begin{cases}\frac{1}{4}n\bar{\upsilon}r_c^2\cdot\frac{2}{\pi}\{\cos^{-1}\frac{\theta}{\theta_0}-\frac{\theta}{\theta_0}(1-\frac{\theta^2}{\theta_0^2})^{\frac{1}{2}}+\frac{2\theta}{3\theta_0}[1-(1-\frac{\theta^2}{\theta_0^2})^{\frac{3}{2}}]\}, 0\le\theta<\theta_0\\ \frac{1}{4}n\bar{\upsilon}r_c^2\cdot\frac{4\theta_0}{3\pi}\cdot\frac{\cos^2\theta}{\sin\theta}, \theta_0\le\theta\le\pi/2\end{cases} \tag{3}$$

where n is the number of atoms per unit volume in the gas chamber, $\bar{\upsilon}$ is the average atomic velocity, θ_0 is the divergence angle of the atomic beam with $\tan\theta_0=2r_c/l$, r_c and l are the radius and length of an oven nozzle aperture that is treated as a point source, respectively.

The dimensional parameters used in this study are shown in Fig. 2. The length l_2 and bore radius r_0 of the hexapole magnet are optimized to maximize the detected atomic beam flux I_{ATOM}, i.e. the total number of detected atoms per second. Taken the spatial distribution and velocity distribution of cesium atoms into consideration, I_{ATOM} can be expressed as:

$$I_{ATOM}=\int_0^{2\pi}\int_0^{\frac{\pi}{2}} I(\theta)(\sum_{\upsilon(\theta)} f(\upsilon)\Delta\upsilon)\cdot\sin\theta d\theta d\varphi \tag{4}$$

where $\upsilon(\theta)$ is the velocity distribution of the detected atoms, which is related to θ, $f(\upsilon)\propto\upsilon^3 e^{-\upsilon^2/\alpha^2}$ is the atomic velocity distribution, α is the most probable velocity.

The calculations of I_{ATOM} and atomic trajectories involve two configurations of oven nozzle apertures: the single channel and multiple channels. For the single channel, with its central x-axis coinciding with that of the hexapole magnet, theoretical equations are employed to attain the atomic trajectories within the hexapole magnetic field. On the other hand, the atomic trajectories within the hexapole magnetic field for the multiple channels were simulated.

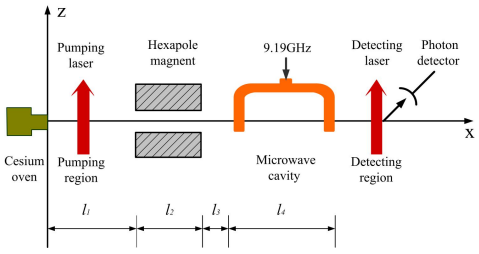

Fig. 2. Schematic diagram of a compact optically pumped cesium beam tube with a hexapole magnetic system, showing dimensional parameters, with the y-axis perpendicular to the plane of the figure.

After leaving the hexapole magnetic field, some atoms would pass through the microwave cavity and enter into the detecting region when their trajectories meet the following boundary conditions that can be applied to both above calculations:

$$\begin{cases} \max(r(x)) < r_0, (r(x) = \sqrt{y(x)^2 + z(x)^2}) \\ -y_b < y(l_3) < y_b, -z_b < z(l_3) < z_b \\ -y_b < y(l_4) < y_b, -z_b < z(l_4) < z_b \end{cases} \quad (5)$$

where $r(x)$ is the radial position of the atoms moving within the magnet, y_b and z_b are half height and width of the microwave cavity entrance, respectively, l_3 is the distance from the magnet exit to the entrance of the microwave cavity, and l_4 is the length of the microwave cavity.

A. The Calculations for The Single Channel

In the case of the single channel, the calculation of atomic trajectories in the hexapole magnetic field can be simplified into deducing variations of the radial displacement r_1 as a function of x. In the hexapole magnetic field, the trajectory equation of the atoms with F=4 state is derived as:*AB*

$$r_1(x) = A\cos\frac{\omega}{\upsilon\cos\theta}x + B\sin\frac{\omega}{\upsilon\cos\theta}x \quad (6.1)$$

$$A = \frac{l_1\tan\theta}{2}\cdot\frac{(1+\cos\frac{2\omega l_1}{\upsilon\cos\theta})}{\cos\frac{\omega l_1}{\upsilon\cos\theta}} - \frac{\upsilon}{\omega}\cdot\sin\theta\cdot\sin\frac{\omega l_1}{\upsilon\cos\theta} \quad (6.2)$$

$$B = l_1\tan\theta\cdot\sin\frac{\omega l_1}{\upsilon\cos\theta} + \frac{\upsilon\sin\theta}{\omega}\cdot\cos\frac{\omega l_1}{\upsilon\cos\theta} \quad (6.3)$$

where l_1 is the distance between the exit of cesium oven and the magnet entrance, υ is the initial velocity of an atom, with $\omega = \frac{1}{r_0}\sqrt{\frac{2\mu_B B_0}{m}}$, μ_B is Bohr's magneton, m is the mass of a cesium atom. Outside the magnetic field, the atoms move in straight line, and their trajectory equation is given by:

$$r_2(x) = r_1(l_1+l_2) + \left.\frac{dr_1(x)}{dx}\right|_{x=l_1+l_2}\cdot x \quad (7)$$

where l_2 is the magnet length, which will be optimized in subsequent calculations.

For the single channel, the atomic trajectories in a cesium beam tube are shown in Fig. 3(a). It can be seen that for those atoms with large emission angle, their trajectories are altered under the hexapole magnetic field, and therefore they are more likely to be detected. The calculation shows that I_{ATOM} reaches the maximum when B_0 is 3.5T. Considering the feasibility in the practical engineering application, B_0 is taken as 1.8T. Figure. 3(b) gives I_{ATOM} versus l_2 as well as r_0, which dependents highly on these two parameters. The optimal values for l_2 and r_0 are found to be 24mm and 2.2mm, respectively, which would enable the most atoms to reach the detecting region. The calculations also indicate that the maximal emission angle θ_{max}=1.93°, below which the atoms can be detected, is much larger than that (0.66°) without the hexapole magnetic system. Figure 3(c) shows the atomic trajectories for the atoms with θ=1.26° and different velocities in the hexapole magnetic field with l_2=24mm. It is noted that the atoms with different initial velocities ranging from 5m/s to 500m/s have diverse periods of the sine wave-like movement. The slower the velocity is, the shorter the period is. As θ increases, more high-velocity atoms would be intercepted.

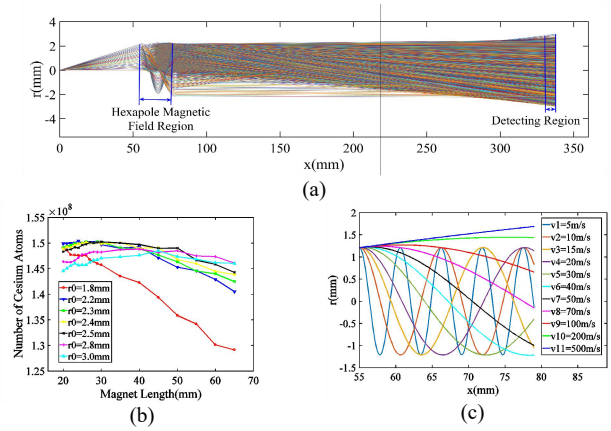

Fig. 3. (a) Atomic trajectories for the single channel. (b) The calculated number of detected atoms using the hexapole magnetic system, for different values of l_2 and r_0. (c) The trajectories of atoms with θ = 1.26° and different velocities in the hexapole magnetic field.

The calculation results of I_{ATOM} per second with m_F=0 state are listed in TABLE I. It can be found that I_{ATOM} with the hexapole magnetic system is about 9.48 times higher than that without the hexapole magnetic system.

TABLE I. CALCULATION RESULTS OF I_{ATOM} PER SECOND WITH m_F=0 STATE FOR THE SINGLE CHANNEL

Without the hexapole magnetic system	With the hexapole magnetic system
1.586×10^7	1.504×10^8

B. The simulations for The multiple Channels

The preliminary calculation for the single channel verifies the effectiveness of the hexapole magnetic focusing method that we proposed. For the multiple channels, the theoretical equations of the single channel are no longer applicable since each channel is situated at a different position. Therefore, the atomic trajectories of each channel were calculated separately to obtain more reliable and accurate results. Typically in a conventional tube, the multiple channel, which are formed by an array of capillary tubes, are stacked into a rectangular shape as shown in Fig. 4.

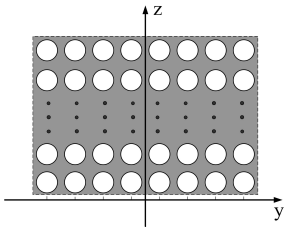

Fig. 4. Arrangement of capillary tubes: a typical one with a rectangular outer shape.

The motion equations for the atoms with F=4 state in the hexapole magnetic field can be expressed as:

$$\ddot{x} = 0 \Rightarrow a_x = 0 \tag{8.1}$$

$$\ddot{r}(x) = -\frac{F}{m} \Rightarrow a_r = -\frac{F}{m} \tag{8.2}$$

where F is defined as (2), a_x is axial acceleration, and a_r is radial acceleration.

In the process of simulation, the length of the magnetic system is divided into the length of equally spaced cells. The direction of the atomic accelerations and velocities at the initial position between each cell were judged, and then different motion trajectory equations were given according to the change of atomic motion states. Figure 5(a) gives the atomic trajectories for the multiple channels. Clearly, the atoms that originally have large emission angles are well focused by the hexapole magnetic field. Figure 5(b) shows the variation of I_{ATOM} for different values of l_2 and r_0. The I_{ATOM}, is found to be higher and flat at l_2 ranging from 33mm to 50mm for r_0=2.8mm, 3.0mm and 3.2mm, while the optimal values of l_2 and r_0 are about 45mm and 2.8mm, respectively. The velocity distributions of the detected cesium atoms with and without the hexapole magnetic system are also simulated, as shown in Fig. 5(c).

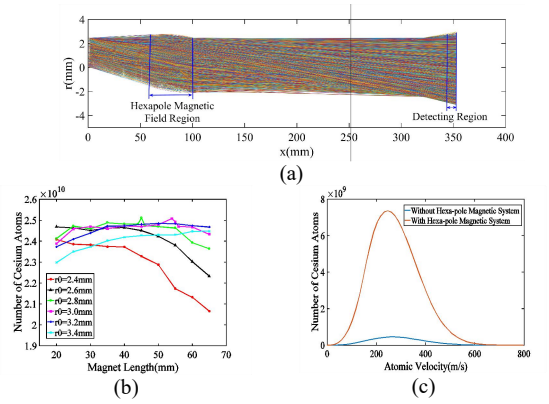

Fig. 5. (a) Atomic trajectories for the multiple channels. (b) The calculated number of detected atoms using the hexapole magnetic system, for different values of l_2 and r_0. (c) Velocity distributions of the detected atoms with and without the hexapole magnetic system.

Table II lists I_{ATOM} per second with m_F=0 state, it can be seen that applying the hexapole magnetic system brings an order of magnitude improvement in the number of detected atoms, which showing an increase of 9.52 times, compared with that without the hexapole magnetic system. It is also found that the atoms with an emission angle $\theta \leq 3.95°$ would be detected, compared to those with a much smaller θ of 0.92° without the hexapole magnetic system. Interestingly, the improvement in the number of the detected atoms for the multiple channels is close to that of 9.48 times calculated for the single channel, further demonstrating the effectiveness of the proposed method. If the detected signal is shot-noise limited, then $S/N = \sqrt{I_{ATOM}}$, which can be found that 3.1 times higher than that without the hexapole magnetic system.

TABLE II. CALCULATION RESULTS OF I_{ATOM} PER SECOND WITH m_F=0 STATE FOR THE MULTIPLE CHANNELS

Without the hexapole magnetic system	With the hexapole magnetic system
2.643×10^{9}	2.517×10^{10}

IV. ENGINEERING DESIGN OF THE HEXAPOLE MAGNETIC SYSTEM

According to the simulation results, the hexapole magnetic focusing method plays an important role in improving the SNR of the optically pumped cesium beam tubes. In order to carry out experimental verification, the solid model of the hexapole magnetic system was engineered. The optimal values for l_2 and r_0 obtained in the simulation of single channel and multiple channels did not consider the space size in the existing optically pumped cesium beam tube, so combined with the existing space structure, l_2 and r_0 were simulated, and the optimal values are 20mm and 3.2mm, respectively.

Taking into account the position fixation between the six limited martingales and the position fixation between the magnetic steel and the fixing device, the solid model of the limited martingale and its fixing device with graphite getters and the solid model of the magnetic steel and its fixing device were designed, respectively, as shown in Fig. 6 and Fig. 7.

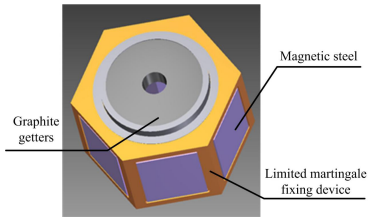

Fig. 6. Solid model of the limited martingale with graphite getters and its fixing device.

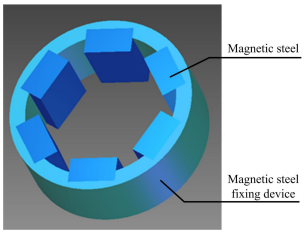

Fig. 7. Solid model of the magnetic steel and its fixing device.

Due to the uneven strong magnetic field generated in the hexapole magnetic system, a magnetic shielding is installed at the exit of this system to eliminate the influence of the hexapole magnetic field on the magnetic field in the microwave cavity, shown as Fig. 8. The hexapole magnetic system is finally fixed to the guide rail in the tube, so the fixing device and baffle connecting the hexapole magnetic system and the guide rail were designed. These two structures ensured the mechanical stability of the hexapole magnetic system during the vibration process, as illustrated in the Fig. 9.

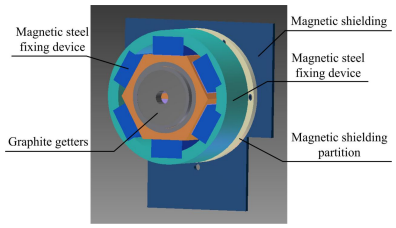

Fig. 8. Solid model of a hexapole magnetic system with a magnetic shielding.

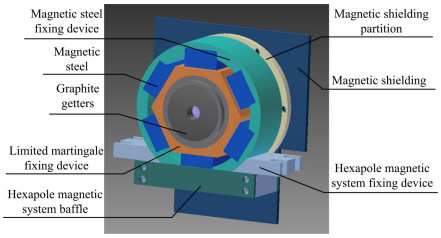

Fig. 9. Complete solid model of a hexapole magnetic system.

Carry out three-dimensional simulation on the designed hexapole magnetic system, the magnetic induction distribution on the connecting line of a pair of magnetic pole cone end is shown in Fig. 10, it can be seen that the magnetic induction at the magnetic pole cone end was about 2.6T, which met the simulation requirements under the condition of multiple channels.

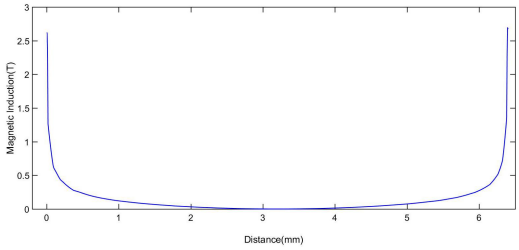

Fig. 10. Distribution of magnetic induction on the connection of a pair of magnetic pole cone end.

In order to verify the effect of the magnetic shielding, Fig. 11 is a schematic diagram of the horizontal and vertical connections of magnetic induction after the magnetic shielding was installed. The simulation is carried out according to the Fig. 11, and the magnetic induction distribution on the horizontal and vertical connections were shown in Fig. 12 and Fig. 13. It can be seen that the maximum values of the horizontal and vertical magnetic induction were only 2 Gauss and 2.2 Gauss, respectively, which achieved the function of shielding the hexapole magnetic field, so that the magnetic field in the microwave cavity would not be interfered by the hexapole magnetic field.

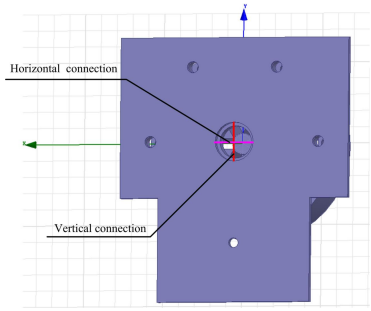

Fig. 11. Schematic diagram of the horizontal and vertical connections of magnetic induction after the magnetic shielding was installed.

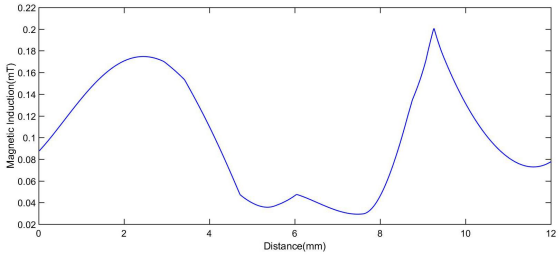

Fig. 12. Distribution of magnetic induction on the horizontal connection.

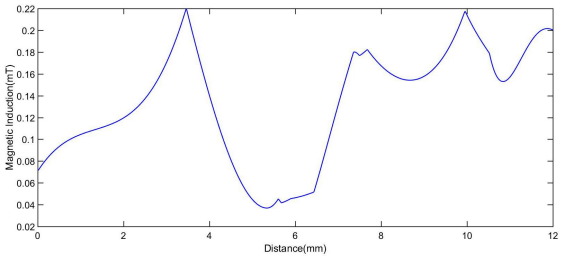

Fig. 13. Distribution of magnetic induction on the vertical connection.

V. DISCUSSION

In multiple channels, along the XOZ plane, Fig. 14 shows a simplified schematic diagram of atomic trajectories when reaching a certain position, where the channels uniformly arranged on Z axis. The signal channel was regarded as the point source at the center of the coordinate axis. However, we considered a number of equally uniformly arranged channels in the multiple channels. As shown in the Fig. 14, the maximum emission angle calculated by the single channel is larger than that calculated by the multiple channels, that is, $\theta_2 > \theta_1$.

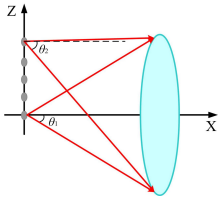

Fig. 14. Simplified schematic diagram of atomic trajectories in multiple channels.

In the calculation of single channel, the atomic trajectories in the hexapole magnetic field was a fixed expression similar to sinusoidal motion derived from the theoretical equation,

however in the multiple channels, considering the true motion state of cesium atoms in the hexapole magnetic field, the length of the hexapole magnetic system was divided into equidistant cells, and the motion states of the atoms in each cell were considered, so as to be closer to the real motion states of cesium atoms, and the equations of atomic trajectories in each cell were different.

Although the hexapole magnetic focusing method provides a new idea for improving the SNR of the optically pumped cesium beam tubes, it is still in a steady beginning stage. Both simulation and engineering design have laid a firm foundation for the fabrication of the compact optically pumped cesium beam tubes using the hexapole magnetic system. The processing of the principle sample tube with a hexapole magnetic system is under way. In the follow-up, we will realize the experimental verification as soon as possible.

VI. Conclusions

In summary, we have performed detailed calculations of the number of the detected cesium atoms and atomic trajectories with the hexapole magnetic system. The number of the detected atoms with $m_F = 0$ state for both single and multiple channel of oven nozzle apertures were found to be 9.5 times higher than that without the focusing system, demonstrating the effectiveness of the hexapole magnetic focusing method proposed in the study. Based on this substantial improvement in the utilization efficiency of cesium atoms, a 3.1 fold increase in the SNR (with assuming all the noises being shot-type) can be predicted, compared with the conventional tubes. Generally known, since the higher the SNR, the better the short-term frequency stability of the cesium beam frequency standards.[31]-[33] The current frequency stability of the high-stability-laser-based optically pumped cesium beam atomic clock $\sigma_y(\tau)=2\times10^{-12}\tau^{-1/2}$[21] is expected to reach a level of $\sigma_y(\tau)=6.7\times10^{-13}\tau^{-1/2}$, comparable to that of NIST-7, if this hexapole magnetic system is adopted. Moreover, with the dual-frequency laser pumping,[34] the above frequency stability may be further increased to $\sigma_y(\tau)=2.2\times10^{-13}\tau^{-1/2}$.

Furthermore, on the basis of simulation, a complete solid model of the hexapole magnetic system was designed, and we verified that the magnetic induction of the designed structure met the simulation requirements under the condition of multiple channels, the interference of the hexapole magnetic field to the microwave cavity was also eliminated.

Acknowledgment

The authors wish to acknowledge valuable technical and theoretical support by many colleagues, with special thanks going to Yiqiu Wang of Peking University.

References

[1] R. C. Hyatt, L. F. Mueller, and T. N. Osterdock, "A high-performance beam tube for cesium beam frequency standards," Hewlett Packard J., vol. 14, 1973, pp.14–23.

[2] J. Vanier and C. Audoin, The quantum physics of atomic frequency standards, CRC Press, Boca Raton, 1989.

[3] A. Bauch, D. Piester, and E. Staliuniene, "A new realization strategy for the time scale," Proc. IEEE Int. Freq. Control Symp. Exhib., p. 518, 2004.

[4] A. Bauch, "The PTB primary clocks CS1 and CS2," Metrologia, vol. 42, 2005, pp. S43– S54.

[5] A. Bauch, K. Dorenwendt, and T. Heindorff, "The PTB's atomic frequency standards CS2 and CSX: frequency shifts by pulling due to neighbouring transitions," Metrologia, vol.24, 1987, pp.199–203.

[6] J. Vanier and C. Audoin, "The classical caesium beam frequency standard: fifty years later," Metrologia vol. 42, 2005, pp. S31–S42.

[7] L. L. Qu, B. Li, and Z. Gao, "Research on the relation between frequency stability and timekeeping clock allocation," 12th IEEE Int. Conf. Electron. Meas. Instrum. (ICEMI), p. 888, 2015.

[8] A. I. Mostafa, G. G. Hamza, and A. Zekry, "Enhancing the frequency stability of national time scale using EMD," IEEE Instrum. Meas. Mag., vol. 23, pp53–60, April 2020.

[9] S. Y. Lin, "A paper clock prediction model for UTC(TL)," Eur. Freq. Time Forum (EFTF), p. 1, 2016.

[10] B. Jaduszliwer, "A cesium beam atomic clock computer model," Proc. IEEE Int. Freq. Control Symp., p. 1097, 1996.

[11] L. Essen and J. V. L. Parry, "An atomic standard of frequency and time interval: a cesium resonator," Nature, vol. 176, 1955, pp. 280–282.

[12] R. E. Drullinger, "Optically pumped primary frequency standards," Proc. 44th Annu. Symp. Freq. Control, p. 76, 1990.

[13] C. Liu, R. Y. Shi, Y. H. Wang, S. Q. Liu, and T. Q. Dong, "An optically detected cesium beam frequency standard with magnetic state selection," Eur. Freq. Time Forum (EFTF), p. 175, 2014.

[14] M. Arditi and J. L. Picque, "A cesium beam atomic clock using laser optically pumping. preliminary tests," J. Phys. Lett. Vol. 41, 1980, pp. L379–L381.

[15] T. Mcclelland, I. Pascaru, J. Zacharski, N.H. Tran, and M. Meirs, "An optically pumped cesium beam frequency standard for military applications," 41st Annu. Symp. Freq. Control, p. 59, 1987.

[16] H. E. Peters, "Magic state selectors in atomic frequency and time standards," Proc. 13th Annu. Precise Time and Time Interval (PTTI) Applications and Planning Meeting, p. 645, 1981.

[17] R. E. Drullinger, J. P. Lowe, D. J. Glaze, and J. H. Shirley, "NIST-7, the new US primary frequency standard," Proc. IEEE Int. Freq. Control Symp., p. 71, 1993.

[18] W. D. Lee, J. H. Shirley, J. P. Lowe, and R. E. Drullinger, "The accuracy evaluation of NIST-7," IEEE Trans. Instrum. Meas., vol. 44, 1995, pp. 120–123.

[19] L. L. Lewis, F. L.Walls, and D. J. Glaze, "Design considerations and performance of NBS-6, the NBS primary frequency standard," Le J. De Physique Colloques, vol. 42, 1981, pp. 241–246.

[20] Y. H. Cao, X. W. Zhao, W. Xie, Q. Wei, L. Yang, H. J. Chen, and S. G. Zhang, "A merchanized optically pumped cesium atomic clock," Jt. Conf. Eur. Freq. Time Forum IEEE Int. Freq. Control Symp. (EFTF/IFCS), p. 618, 2017.

[21] H. S. Shang, T. Y. Zhang, J. X. Miao, T. T. Shi, D. Pan, X. W. Zhao, Q. Wei, L. Yang, and J. B. Chen, "Laser with 10^{-13} shotr-term instability for compact optically pumped cesium beam atomic clock," Opt. Express, vol. 28, 2020, pp. 6868–6880.

[22] G. Breit and I. I. Rabi, "Measurement of nuclear spin," Phys. Review, vol. 38, 1931, pp. 2082–2083.

[23] H. M. Goldenberg, D. Kleppner, and N. F. Ramsey, "Atomic hydrogen maser," Phys. Rev. Lett. Vol. 5, 1960, pp. 361–362.

[24] L. Essen, R. W. Donaldson, E. G. Hope, and M. J. Bangham, "Hydrogen maser work at the national physical laboratory," Metrologia, vol. 9, 1973, pp. 128–137.

[25] J. B. Chen, F. Z. Wang, Y. Q. Wang, and D. H. Yang, "A. New Design of a Diffused Laser Light Optically Pumped Small Cesium Beam Frequency Standard," IEEE Trans. Ultrason., Ferroelectr., Freq. Control, vol. 47, 2000, pp. 457–460.

[26] S. E. Park, H. Cho, S. H. Yang, and H. S. Lee, "A continuous slow atomic beam for a cesium frequency standard," Conf. Precis. Electromagn. Meas. Conf. Digest (CPEM), p. 627, 2000.

[27] G. Avila, V. Giordano, V. Candelier, E. D. Clercq, G. Theobald, and P. Cerez, "State selection in a cesium beam by laser-diode optical pumping," Phys. Rev. A, vol. 36, 1987, pp. 3719–3728.

[28] K. Hagimoto, S. Ohshima, Y. Nakadan, and Y. Koga, “Accuracy evaluation of the optically pumped Cs frequency standard at NRLM,” IEEE Trans. Instrum. Meas, vol. 48, 1999, pp. 496–499.

[29] W. D. Lee, J. H. Shirley, D. A. Jennings, T. E. Parker, S. R. Jefferts, and R. E. Drullinger, “An atomic beam velocity servo for optically pumped cesium frequency standards,” Proc. IEEE Int. Freq. Control Symp., p. 1082, 1996.

[30] J. A. Giordmaine and T. C. Wang, “Molecular beam formation by long paralllel tubes,” J. Appl. Phys, vol. 31, 1960, pp. 463–471.

[31] R. F. Lacey, A. L. Helgesson, and J. H. Holloway, “Short-term stability of passive atomic frequency standards,” Proc. IEEE. Vol. 54, 1966, pp. 170–176.

[32] K. Hisadome and M. Kihara, “Short-Term Frequency Stability Estimation of an Optically Pumped Cesium Beam Frequency Standard,” Jpn. J. Appl. Phys., vol. 33, 1994, pp. 1669–1673.

[33] V. Candelier, V. Giordano, A. Hamel, G. Theobald, P. Cerez, and C. Audoin, “Frequency stability of an optically pumped cesium beam frequency standard,” Appl. Phys. B, vol. 49, 1989, pp. 365–370.

[34] G. Avila, E. De Clercq, M. De Labachellerie, and P. Cérez, “Microwave Ramsey resonances from a laser diode optically pumped cesium beam resonator,” IEEE Trans. Instrum. Meas. Vol. IM-34, 1985, pp. 139–143.